Virtual FFR quantified with a generalized flow model using Windkessel boundary conditions ; Application to a patient-specific coronary tree.

Keltoum Chahour, Rajae Aboulaich, Abderrahmane Habbal, Nejib Zemzemi, Cherif Abdelkhirane

Noname manuscript No.
(will be inserted by the editor)

Virtual FFR quantified with a generalized flow model using Windkessel boundary conditions

Application to a patient-specific coronary tree

Keltoum Chahour[1,2,⋆] · Rajae Aboulaich[1] · Abderrahmane Habbal[2] · Nejib Zemzemi[3] · Chérif Abdelkhirane[4]

Received: date / Accepted: date

Abstract Fractional flow reserve (FFR) has proved its efficiency in improving patients diagnosis. In this paper, we consider a 2D reconstructed left coronary tree with two artificial lesions of different degrees. We use a generalized fluid model with a Carreau law and implement the Windkessel boundary conditions at the outlets. We introduce our methodology to quantify the FFR, and lead several numerical experiments. For two different finite element meshes, we compare the FFR results for Navier Stokes versus generalized flow models, and for Windkessel versus free outlets boundary conditions. We also used mixed boundary conditions. Our results highlight the fact that free outlets boundary conditions are sensitive to the FFR sensor position. The computational FFR results show that the degree of stenosis is not enough to classify a lesion, while there is a good agreement between Navier Stokes and generalized flow model in classifying the lesions.

Keywords Generalized flow model · Fractional flow reserve · Windkessel model.

1 Introduction

The coronary arteries are a common and important site of the development of sclerotic lesions. Thus, a detailed hemodynamic evaluation of the flow and its spatial and temporal distribution may give important insight to understand the progression of atherosclerosis, which has a useful clinical value. In this view, the fractional flow reserve (FFR) plays a central role, see [13]. The fractional flow reserve (FFR) is an invasive measure that consists in introducing a pressure wire to a diseased artery to measure in vivo two values of blood pressure : the aortic pressure P_{aortic}, and the pressure distal to a lesion, P_{distal}. These pressure values are then used to calculate the FFR ratio. According to the value obtained, the clinician decides whether the lesion is hemodynamically significant (FFR lower than 0.80) or non-significant (FFR higher than 0.80). In the case of a significant lesion, a revascularization is necessary. In this case, a realistic simulation of vascular blood flow inside the coronary arteries can be a better alternative to the invasive FFR, see [2] and [18] . On the one hand, a realistic blood flow simulation requires the use of an adequate flow model. For instance, Boujena and al. [2] presented a Non Newtonian flow model adapted to describe blood flow in the presence of atherosclerosis. Simulation in their paper was performed in 2D and 3D

⋆ Corresponding author : keltoumchahour@gmail.com.

[1] LERMA, Mohammadia Engineering School, Mohamed V University in Rabat, Morocco.
[2] LJAD Université Côte d'Azur, Parc Valrose, 06108 Nice, France.
[3] INRIA Bordeaux Sud Ouest, Carmen Project, France.
[4] Department of Interventional Cardiology, Clinique des spécialités Achifaa, Casablanca, Morocco.

simplified geometries. On the other hand, the choice of suitable boundary conditions is crucial. In our previous paper [13], we presented a first virtual FFR estimation using the generalized fluid model in [2] and led different simulations to study the impact of the lesions parameters on the FFR value. However, we considered a simplified 2D geometry and reduced boundary conditions. In this paper, the domain of simulation corresponds to a realistic diseased coronary tree with many outlets. Thus, we address a special concern to the boundary conditions model. In fact, the shape and the type of the function at the inlet are determinant of the flow and pressure patterns obtained in the domain. In the case where the study aims at comparing the results to in vivo measurements, the inlet boundary condition should be adequately chosen. Many works explored the effect of the inlet boundary condition, among them Liu and al. [4] and Taylor and al. [3] presented realistic forms of inlet boundary condition in the case of coronary blood flow. Concerning the outlet, the most common boundary condition for blood flow correspond to a constant pressure. However, this choice is not realistic when it comes to complex geometries, with many outlets. The strategy of resolution in this case consists in dividing the domain into two parts : the upstream domain, and the downstream domain that includes the outlets. The outlet boundary conditions are defined in the downstream domain using an appropriate model, usually based on an electrical analogy, known as the Windkessel effect, see [5] and [6]. In the first section, we give the essential elements for simulation : the 2D multi-stenotic domain defined using segmentation techniques, the realistic flow model and finally suitable boundary conditions. In the second section, we present the pressure and the flow distributions obtained for three different outlet boundary conditions. Finally, in the last section, we give an estimation of the fractional flow reserve (FFR) for two lesions using the pressure pattern in the stenotic coronary tree. The FFR calculation is performed using two different flow models: Navier Stokes and the generalized flow model, and considering diverse outlet boundary conditions.

2 Methods

2.1 Domain definition: 2D image segmentation

In order to create a realistic geometry for numerical simulation, we started from a 2D patient specific angiography. An enhancement technique was done before this image could be segmented. In this phase, different filters were used to improve the contrast of the original image, see [15]. Then opening/closing Matlab functions were used to extract a black and white image that contains only the coronary tree in which we are interested. It should be noticed that despite the fact that the original angiography corresponds to a stenotic coronary tree, due to the lower quality of the image, and to the small degree of stenosis of the lesion, this last could not appear in the black and white image. Since our aim in this paper is to investigate the impact of the flow model and the boundary conditions on the FFR, we introduced two different artificial lesions in the coronary tree. The first lesion corresponds to 68% stenosis and was drawn in the same location of the real patient's lesion. The second lesion corresponds to 56% stenosis and was drawn at the entrance of the longest branch in the coronary tree. This choice is justified by the purpose of calculating the fractional flow reserve in the case of free outlet boundary conditions. The resulting 2D multi-stenotic domain, the original extracted tree, and the original angiography are given in figure 1.

Starting from the new multi-stenotic coronary tree, the segmentation and the meshing were performed later using a homemade Freefem++ code, see [7].

2.2 Coronary blood flow model

The blood was assumed as an incompressible, non-Newtonian viscous fluid obeying the Carreau law with the viscosity shear rate relation given by :

$$\mu = \mu_\infty + (\mu_0 - \mu_\infty)(1 + (\lambda s(u))^2)^{(n-1)/2} \tag{1}$$

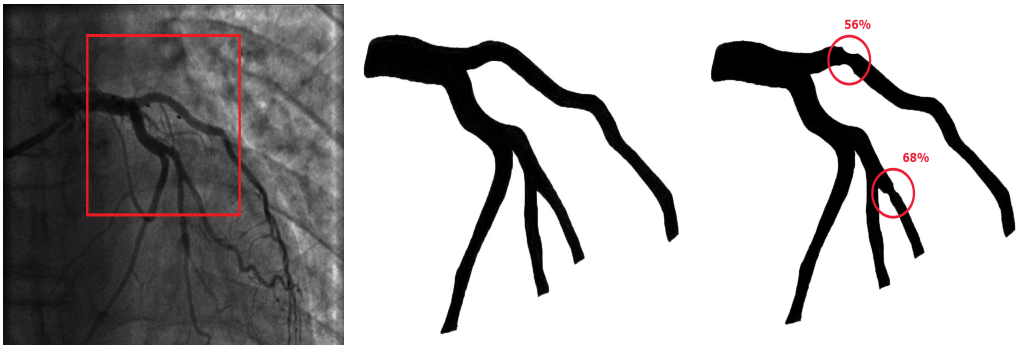

Fig. 1 From left to right: The original angiography image, the coronary tree of interest is framed with red. The Black and white original image. The resulting multi-stenotic coronary tree.

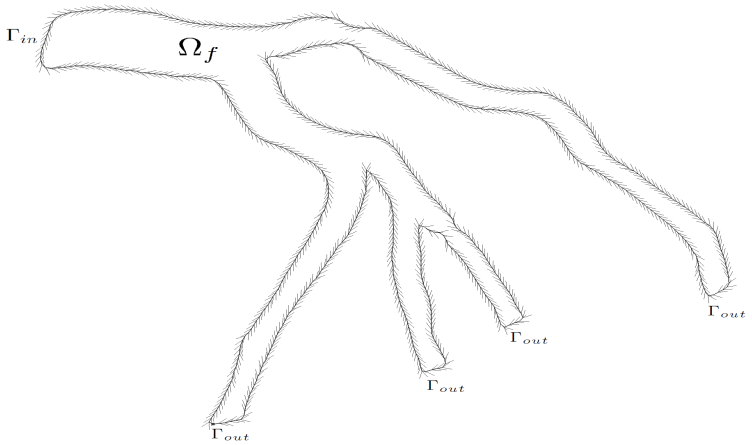

Fig. 2 The 2D geometry considered. Arrows indicate the isoline orientation.

where $\mu_0 = 0.0456 \ \ Pa.s$ and $\mu_\infty = 0.0032 \ \ Pa.s$ are the values of the viscosity for the lowest and highest shear rates. The parameters values $\lambda = 10.03s$ and $n = 0.344$ are typical for the Carreau law. The shear rate $s(u)$ is defined as follows:

$$(s(u))^2 = 2Du : Du = 2\sum_{i,j}(Du)_{ij}(Du)_{ji} \tag{2}$$

with :

$$Du = \frac{1}{2}(\nabla u + \nabla^T u) \tag{3}$$

The geometrical 2D domain Ω_f is given in figure 2. The time dependent two dimensional generalized fluid equations presented in [1] were considered as the governing equations in the tree domain Ω_f :

$$\begin{cases} \rho_f \dfrac{\partial u}{\partial t} + \rho_f (u.\nabla)u - \nabla.(2\mu(s(u))Du) + \nabla p = 0, \ \ in \ \ \Omega_f \times (0,T_c) \\ \nabla.u = 0, \ \ in \ \ \Omega_f \times (0,T_c) \end{cases} \tag{4}$$

where u is the incompressible velocity and p is the pressure. In the computations, the blood density ρ_f was assumed to be constant at 1060 $\ Kg.m^{-3}$. A

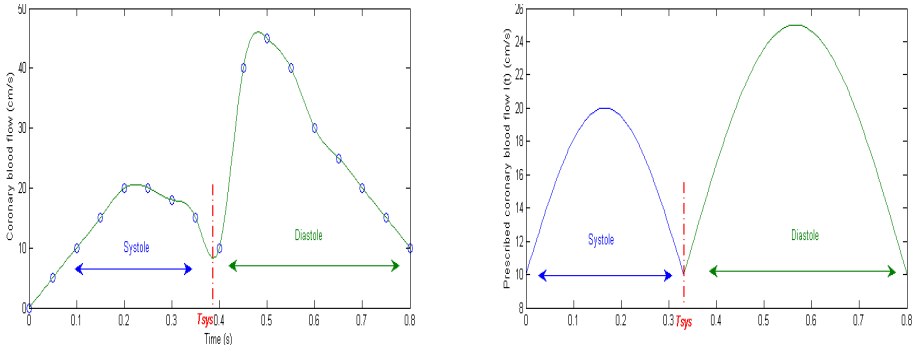

Fig. 3 Left, spline function approaching left coronary blood flow. Right, the flow function prescribed at the inlet $I(t)$.

no-slip condition was applied to the velocities at the lumen wall, considered to be inelastic and impermeable. A steady Stokes initial condition, with a Poiseuille function at the inlet was imposed. T_c corresponds to the duration of a cardiac cycle under normal conditions, we took $T_c = 0.8s$ (corresponding to a heart rate of 75 beats per minute).

2.3 Boundary conditions : Inlet / Outlets

Since the processed image treated corresponds to a left coronary artery, we used sinusoïdal functions to approach the inlet flow distribution into the left coronary artery. The shape of this function is well known, see [4]. Considering that T_{sys} is the period of systole, t_s the start of the systolic phase of the current cardiac cycle and t_d the start of the diastolic phase, this periodic function $I(t)$ can be written as follows:

$$I(t) = \begin{cases} (I_p + I_0 * sin(\pi * (t - ts)/Tsys), 0), & 0 \leq t \leq T_{sys} \\ (I_p + I_c * sin(\pi * (t - td)/(T_c - Tsys)), 0), & T_{sys} \leq t \leq T_c. \end{cases} \tag{5}$$

where $I_p = 10\ cm/s$ represents the dominant flow, $I_0 = 10\ cm/s$ and $I_c = 10\ cm/s$. T_{sys} is taken equal to 0.33s. The remaining duration from the cardiac cycle corresponds to a diastole. The profile of this function is given in figure 3.

To assess the influence of outlet boundary conditions on the pressure and flow fields, two different outlet boundary conditions were utilized in this study: free pressure and a 2 elements Windkessel model [6] to incorporate the resistant effect of the downstream bed. In order to comply to the physics of the downstream domain, additional terms have to be added to the flow model. At this level, we need to introduce the two operators: $M = [M_m, \overrightarrow{M_c}]$ and $H = [H_m, \overrightarrow{H_c}]$. Each one of M and H is composed of a momentum and a continuity operator respectively. They are defined at the outlets based on the chosen model to represent the downstream domain, see [6]. In this paper, we opted for a Windkessel model. The variational formulation of our problem in this case can be written as follows:

$$\begin{cases} \rho_f \int_{\Omega_f} \frac{\partial u}{\partial t} v dx + (Au, v) + \rho_f b(u,u,v) - \boxed{\int_{\Gamma_{out}} v.(M_m(u,p) + H_m(u,p)).\overrightarrow{n}\, ds} \\ \quad + \boxed{\int_{\Gamma_{out}} q.(\overrightarrow{M_c}(u,p) + \overrightarrow{H_c}(u,p)).\overrightarrow{n}\, ds} = 0, \ \ \forall v \in V, \forall p \in P \\ u = I(t), \ \ in \ \ \Gamma_{in} \\ u(0) = u_0, \ \ in \ \ \Omega_f \end{cases} \tag{6}$$

with :

$$(Au, v) = \int_{\Omega_f} 2\mu(s(u)) Du : Dv dx, \tag{7}$$

$$b(u,v,w) = \sum_{i,j=1}^{2} \int_{\Omega_f} u_i \frac{\partial v_j}{\partial x_i} w_j dx \tag{8}$$

The expressions of the boxed terms are given in the next section.

2.4 The Windkessel model

The Windkessel model (or the lumped parameter model) was originally derived by the physiologist Otto Frank in an article published in 1899 [8] to describe the afterload of the heart related to pumping blood through the arterial system, as described in [6]. It is based on an electrical analogy where an arterial tree is assimilated to an electric circuit. The parameters of the components of the circuit (resistances, capacitances, etc) correspond to the properties of each branch. The variables are the voltage at every node and the current in each branch. In the context of blood flowing in an arterial network, pressure plays the role of voltage and flow rate the role of current. During a cardiac cycle, a 2 elements Windkessel model takes into account the effect of arterial compliance and total peripheral resistance. In the electrical analogy, the arterial compliance (C in $cm^3/mmHg$) is represented as a capacitor with electric charge storage properties. Peripheral resistance of the systemic arterial system (R in mmHg s/cm^3) is represented as an energy dissipating resistor. The flow of blood in the heart (I(t) in cm^3/s) is analogous to that of current flowing in the circuit and the blood pressure ($P_d(t)$ in mmHg) is modeled as a time-varying electric potential. Figure 4 gives a schematic view of the circuit. The theoretical modeling as seen in the electrical analogy is given by the equation:

$$I(t) = \frac{P_d(t)}{R} + C\frac{dP_d(t)}{dt}$$

Thus, and as proved in [6], the operators M and H are defined so that the boxed terms introduced in the previous section are defined as follows, where $P_d(t)$ is a solution to the electrical equation above:

$$\begin{aligned} &\int_{\Gamma_{out}} v.M_m(u,p).\overrightarrow{n}\, ds \\ &\qquad = -\int_{\Gamma_{out}} v.\overrightarrow{n} \ \ (R\int_{\Gamma_{out}} u.\overrightarrow{n}\, ds + \int_0^t \frac{e^{-(t-t_1)}/\delta}{C} \int_{\Gamma_{out}} u(t_1).nds.dt_1 + \overrightarrow{n}.\tau.\overrightarrow{n}) \ \ ds \\ &+ \int_{\Gamma_{out}} v.\tau.\overrightarrow{n}\, ds \end{aligned} \tag{9}$$

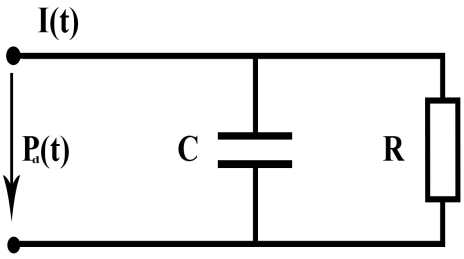

Fig. 4 Windkessel electrical analogy.

$$\int_{\Gamma_{out}} v.H_m(u,p).\overrightarrow{n}\,ds$$
$$= -\int_{\Gamma_{out}} v.\overrightarrow{n}\ \ ((P(0)-R\int_{\Gamma_{out}} u(0).\overrightarrow{n}\,d\Gamma - P_d(0))e^{-t/\delta}+P_d(t))\ \ ds \tag{10}$$

where $\delta = RC$, $R = 0.95$ and $C = 1.06$. After the resolution of our problem using a finite element method under FreeFem++, we obtain the numerical results presented in the next section.

2.5 Fractional flow reserve (FFR)

The fractional flow reserve is crucial to quantify the hemodynamic severity of the stenosis in the case of intermediate lesions, where the degree of stenosis varies between 40% and 70%, see [10]. From a clinical standpoint, this measure indicates the degree of implication of stenosis in ischemia, that is a deficient supply of oxygen to the myocardium.

To measure the fractional flow reserve (FFR) during the invasive test, the operator crosses the coronary lesion with an FFR-specific guide wire. This guide wire is designed to record the coronary arterial pressure beyond the lesion (figure 5 left). Once the transducer is distal to the lesion (approximately 20 mm), a hyperemic stimulus is administered by injection through the guiding catheter. The maximal hyperemia should be reached to avoid underestimating the value of FFR, see [9]. The mean arterial pressures from the pressure wire transducer P_{aortic} and from the guide sensor P_{distal} are then used to calculate FFR ratio: $FFR = \frac{P_{distal}}{P_{aortic}}$ (figure 5 right). The aortic pressure P_{aortic} is the central blood pressure at the root of the aorta, while the distal pressure P_{distal} corresponds to the pressure at the surface of the sensor (pressure wire in figure 5 left). Both pressures given by the FFR instrument are calculated as a temporal mean, over the cardiac cycle, of pressures $p_s(t)$ captured at each frequency drop, see [13]. These pressures can be written as follows:

$$P = \frac{1}{T_c}\int_0^{T_c} p_s(t)dt \tag{11}$$

An FFR value lower than 0.75 indicates a hemodynamically significant lesion. An FFR value higher than 0.8 indicates a lesion that is not hemodynamically significant. Values between 0.75 and 0.80 are critical. In this case, the FFR is not a reliable element in clinical decision-making.

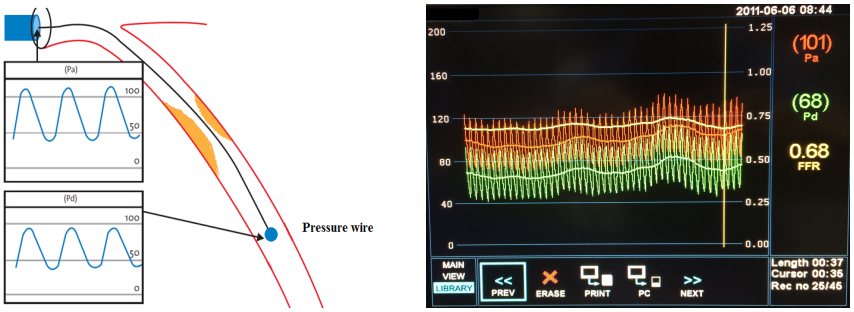

Fig. 5 Left, schema of the invasive FFR technique. Right, a typical example of FFR measurement. Automated calculation of FFR (*yellow*) corresponds to the ratio of mean distal coronary pressure (*green*) to mean aortic pressure (*red*) during maximal hyperemia.

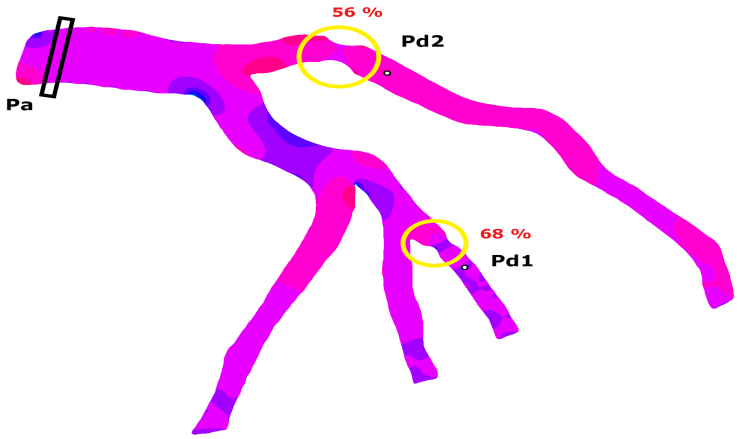

Fig. 6 FFR calculation. The mutli-stenotic coronary tree contains two lesions: 56% stenosis and 68% stenosis.

Our objective is to give an estimation of the FFR for both lesions in the diseased coronary tree using the pressure distributions obtained in the tree domain. We aim at the study of the effect of the flow model and the outlet boundary conditions on the FFR value. For this reason, we consider two different flow models: Navier Stokes versus the generalized flow model (presented in the previous section), and three options for outlets boundary conditions: Windkessel, free outlets and mixed boundary conditions given in detail in the next section. We assume that the 2D geometry for FFR measurements corresponds to a maximal vasodilation. In fact, a clinically certified FFR value (compared to real FFR measurements) is not our ultimate goal in this paper. We implement an algorithm to comput a virtual FFR following the same calculation strategy as used by the clinical FFR device, like in [13]. At each time step, the aortic pressure P_a is calculated by the mean pressure of the points at 1 cm from the inlet of the coronary tree, in order to avoid all the transient effects at the entrance.

The distal pressure P_d is obtained at a distance of 1 cm beyond each lesion on the sensor contour assimilated to a disk with constant diameter. The ratio between the sensor diameter and the reference diameter of the branch is: $\frac{D_{sensor}}{D_{ref}} = \frac{1}{10}$, based on the common magnitude of the sensor diameter that is $0.014'' = 0.35$ mm. It should be noticed that the 2D disk is not virtuel and is considered as an obstacle to the flow, in contrast to the virtual box for P_a calculation. The diagram in figure 6 describes the approach. At each cardiac cycle - and during five consecutive cardiac cycles - a temporal mean pressure of P_a and

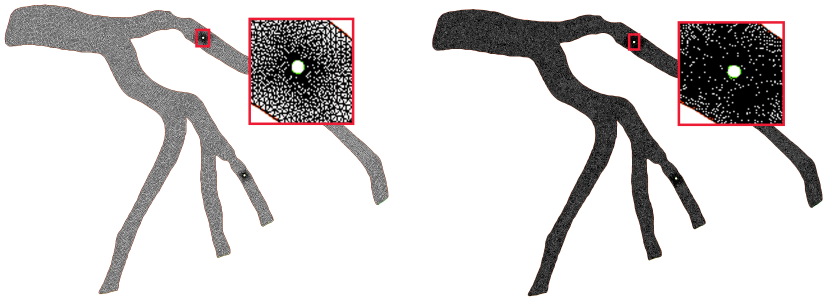

Fig. 7 Plot of the two meshes used for simulations: 14240 nodes vs 55353 nodes.

P_d is performed. The ratio of these two pressures gives an FFR value at each cardiac cycle. In order to increase the precision of the computed FFR, we used two different finite element meshes given in figure 7.

3 Results

3.1 Numerical results

Simulations are performed using the finite element solver Freefem++, based on an explicit time discretization scheme. Fluid velocity and pressure are calculated at each time step. The time step used is $\delta t = 5.10^{-3}\ s$ and the duration of a cardiac cycle is $T_c = 0.8\ s$. Five consecutive cardiac cycles were simulated to reach a periodic regime of the flow. As for the spatial discretization, two different sizes of mesh were considered: the first mesh file contains 14240 elements, and a second mesh which contains 55353 elements is obtained by using a split command. The global layout of the solution was not modified, but the values for the velocity and pressure in each element were slightly different. That explains the variation in the FFR values given in table 1 (last section). This is mainly due to the curved aspect of the 2D domain and to the fact that the common finite element method is not well-adapted in our case, see [12]. Moreover, it is recognized that the numerical resolution of the Non Newtonian Navier Stokes equation is sensitive to the mesh size and to mesh modification.

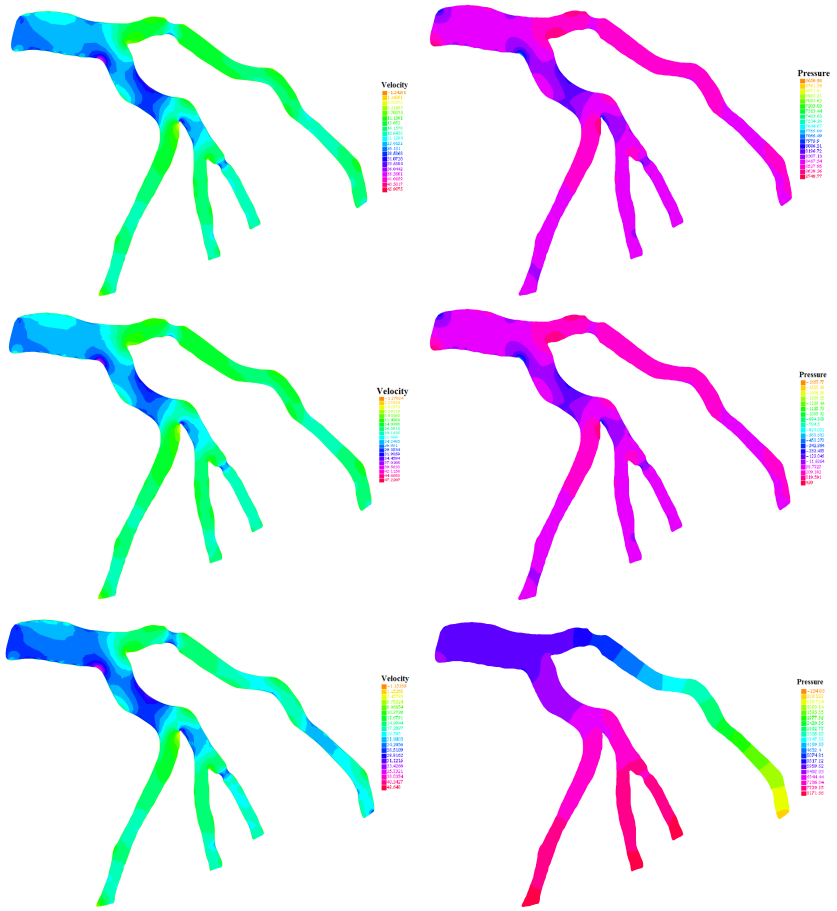

Fig. 8 From top to bottom: Velocity and pressure fields at $t = 0.59s$ (peak diastole) using Windkessel model, free pressure outlet boundary conditions and mixed outlet boundary conditions (as defined in the paragraph above) respectively.

The results in figure 8 give the flow (magnitude of velocity) and pressure patterns into the stenotic coronary artery at the peak diastole of the first cardiac cycle. The same flow model - Non Newtonian Navier Stokes - is used for all simulations. As for the inlet, the same boundary condition that is introduced in the first section is adopted, see figure 3. However, three different outlet boundary conditions were considered: firstly, we considered that the whole coronary tree corresponds to a 2 elements Windkessel model. Secondly, we used a free pressure boundary condition for all the outlets. Finally, we introduced mixed outlet boundary conditions where the longest stenotic branch of the tree is considered as a free outlet, and the remaining three branches corresponds to a 2 elements Windkessel model.

3.2 Fractional flow reserve (FFR) computation

The lesions of interest have a degree of stenosis equal to 56% and 68%, which makes them both in the intermediate value range. That justifies the necessity of the fractional flow reserve in taking a clinical decision. Table 1 gives the FFR values for these two lesions using Navier Stokes and the generalized flow model and considering three different options for the outlet boundary conditions: Windkessel model, free

Mesh size	Coarse mesh					
Flow model	Navier Stokes			Generalized flow		
Outflow BC	Wind-kessel	Free Outlet	Mixed BC	Wind-kessel	Free Outlet	Mixed BC
FFR 1	0.760	0.119	0.885	0.7478	0.106	0.8567
FFR 2	0.917	0.710	0.717	0.908	0.698	0.722
Mesh size	Fine mesh					
Flow model	Navier Stokes			Generalized flow		
Outflow BC	Wind-kessel	Free Outlet	Mixed BC	Wind-kessel	Free Outlet	Mixed BC
FFR 1	0.8205	0.2459	0.9891	0.8039	0.2082	0.9791
FFR 2	0.9515	0.8704	0.7172	0.9404	0.8096	0.7229

Table 1 FFR values for both lesions correponding to the two flow models and the different outlet boundary conditions. The two mesh files presented in figure 7 were used for these calculations.

outlets and mixed outlet boundary conditions where only the longest branch is considered free while the other branches are assimilated to a 2 elements Windkessel model. The FFR result in table 1 corresponds to the mean FFR during five cardiac cycles in each different case of study. As mentioned in the previous section, our model and thus the algorithm of FFR estimation are sensitive to the mesh discretization. In this view, we consider that the finer mesh provides a better estimation of the FFR as it better approximates the 2D curved domain. Consequently, the analysis of the different results in table 1 is based on the finer mesh simulations.

4 Discussions

Results in figure 8 show that the velocity and pressure fields have approximately the same layout with Windkessel and free outlets boundary conditions even if the isovalues are different. This is due to the fact that in both these cases no one of the outlets is advantageous comparing to the others (resistive effect or free exit in all of them). In contrary, with mixed boundary conditions, the longuest branch is free while the rest corresponds to a 2 element Windkessel model. As a result, we observe lower values of pressure in this branch and eventually higher values of velocity which is completely intuitive.

The flow model considered for simulations is only slightly influencing the FFR value. For example, considering the possible options for outlets boundary conditions, the difference in the FFR between the Navier Stokes model and the non-Newtonian flow model does not exceed 2% where the outlets are not all free. In the case of free outlets, the decrease in the FFR value for the first lesion is quite surprising (cells in gray in the table): up to 79% and 75% with the generalized fluid and the Navier Stokes models respectively. In fact, there is a huge pressure drop in the P_d value since the distal sensor for this lesion is not far enough from the free exit. In the contrary, we do not have this problem with the second lesion as the branch is long enough beyond the sensor. That shows that this type of boundary conditions are not appropriate and not realistic to perform a such calculation in the coronary arteries, though their widespread use, see [14]. Now, comparing between Windkessel and mixed boundary conditions, we can see that the first lesion conserves the same FFR classification - hemodynamically non-significant - while the second lesion moves from the non- significant stenosis class to the significant one. These same classifications are conserverd with both flow models.

Considering the fact that the first lesion has an important degree of stenosis (68%) while the second one is a 56% lesion, this result confirms that the FFR value is not only depending on the degree of stenosis, which renders a physical severity of the lesion, but also on the haemodynamical flow inside the connected tree, strongly impacted by the flow model and the nature of boundary conditions (inlets and especially outlets boundary conditions).

5 Conclusions

In recent decades, much progress has been made in research coupling medical imaging and computational fluid dynamics to study cardiovascular hemodynamics, see [11]. The developed methods could provide clinicians with powerful new tools, rivaling and even surpassing experimental fluid mechanics methods to investigate the mechanisms of disease and to design medical devices and therapeutic interventions. The obtention of clinically useful numerical results is not possible without the combination of different elements. On one hand, realistic models, suitable boundary conditions, and realistic domains for simulation. On the other hand, the interaction between clinicians and mathematicians is compulsory in terms of assessment and definition of new problematics.

In this work we calculated the fractional flow reserve (FFR) corresponding to a multi-stenotic patient specific coronary tree. The two lesions of interest were not present in the original angiography, but were incorporated artificially into the tree in the same way a lesion appears in the X-ray angiography. Thus, the used geometry is enough realistic to represent important features of the flow in a real diseased coronary tree. The two intermediate lesions of interest have degrees of stenosis of 68% and 56%. The FFR classification for these two lesions was not sensitive to the flow model adopted for the simulation even if the FFR value were slightly different between the Navier Stokes and the non-Newtonian flow model. However, according to the chosen option for outlets boundary conditions we could have a different lesion classification. Based on the finer mesh simulations, the second lesion moved from the insignificant to the significant value range stenosis. Based on the simulation results, we summarize following conclusions:

- There is a good agreement between Navier Stokes and the generalized flow model in simulating coronary blood flow and thus in classifying coronary lesions provided fluid parameters are appropriate, see [17].
- Free outlet boundary conditions are not realistic to consider for FFR computation, since they are sensitive to the FFR sensor position. Moreover, they do not reproduce the resistant effect of the coronary downstream bed. In contrary to the Windkessel model even if the parameters R and C are taken constant.
- The study confirms the fact that the degree of stenosis is not enough to quantify the severity of a lesion, see [16]. In our case, the two considered lesions had different classifications in each time outlet boundary conditions were modified.

Our aim was to place emphasis on the sensitivity of the FFR calculations and flow features in coronary arteries to the physical model, the boundary conditions and the space discretization as well, keeping out of scope the important purpose of validating virtual FFR against clinical data. Indeed, the FFR value issued from a 2D simulation can not be directly compared to the real invasive FFR, since a 2D angiography based reconstruction of the coronary tree is not the best representation of the physiological domain. This is principally due to branch torsion and to transient movements induced by the respiratory system during image recording. As a result, one perspective to this work is the reproduction of the coronary blood flow into a 3D geometry, see [11].

Thanks

This work has been supported by EPICARD cooperative research program, funded by INRIA international laboratory LIRIMA. This study received financial support from the French Government as part of the Investments of the future program managed by the National Research Agency (ANR), Grant reference ANR-10-IAHU-04-LIRYC.

References

1. Boujena S, Kafi O, El Khatib N (2014) Generalized Navier–Stokes equations with non-standard conditions for blood flow in atherosclerotic artery. Applicable Analysis 95(8):1645-1670. https://doi.org/10.1080/00036811.2015.1068297

2. Morris D, Van de Vosse N, Lawford V, Rodney Hose D, Gunn P (2015) Virtual (Computed) Fractional Flow Reserve : Current Challenges and Limitations. *Elsevier JACC Cardiovasc Interv 8(8): 1009–1017.* https://doi.org/10.1016/j.jcin.2015.04.006

3. Taylor CA, Steinman DA (2010) Image-based modeling of blood flow and vessel wall dynamics: Applications, Methods and Future Directions. *Ann Biomed Eng 38(3):1188-203.* https://doi.org/10.1007/s10439-010-9901-0

4. Liu B, Zheng J, Bach R, Tang D (2015) Influence of model boundary conditions on blood flow patterns in a patient specific stenotic right coronary artery. *BioMed Eng OnLine 14(Suppl 1): S1.* https://doi.org/10.1186/1475-925X-14-S1-S6

5. Catanho M, Sinha M, Vijayan V (2012) Model of Aortic Blood Flow using the Windkessel Effect. Report : BENG 221 - Mathematical Methods in Bioengineering. http://isn.ucsd.edu/classes/beng221/problems/2012/BENG221_Project - Catanho Sinha Vijayan.pdf

6. Vignon-Clementel IE (2006) A coupled multidomain method for computational modeling of blood flow. Phd thesis, Department of mechanical engineering, Stanford university. https://team.inria.fr/reo/files/2012/07/Vie-thesis-asInStanford.pdf

7. Hecht F (2006) Freefem++ Documentation. https://freefem.org/#documentation

8. Frank O (1899) Die Grundform des arteriellen pulses: Mathematische Analyse. Erste Abhandlung. *Zeitung für Biologie.*

9. Toth G, Johnson P, Jeremias A, Pellicano M, Vranckx P, Fearon F, Barbato E, Kern J, Pijls N, Bruyne (2016) Standardization of Fractional Flow Reserve Measurements. *J Am Coll Cardiol 68(7):742-53.* https://doi.org/10.1016/j.jacc.2016.05.067

10. Cuisset T, QuiliCi J, Cayla G (2013) Qu'est-ce que la FFR ? Comment l'utiliser ? *Réalités Cardiologiques 291.* http://www.realites-cardiologiques.com/wp-content/uploads/sites/2/2013/02/11.pdf

11. Javadzadegan, Yong AS, Chang M, Ng AC, Yiannikas J, Ng MK, Behnia M, Kritharides L (2013) Flow recirculation zone length and shear rate are differentially affected by stenosis severity in human coronary arteries. *Am J Physiol Heart Circ Physiol 304(4):H559-66.* https://doi.org/10.1152/ajpheart.00428.2012

12. Shepharda MS, Flaherty J, Jansena K, Li X, Luo X, Chevaugeon N, Remacle JF, Beall M, O'Barac RM (2005) Adaptive mesh generation for curved domains. Applied Numerical Mathematics *52:251–27.* https://doi.org/10.1016/j.apnum.2004.08.040

13. Chahour K, Aboulaich R, Habbal A, Abdelkhirane C, Zemzemi N (2018) Numerical simulation of the fractional flow reserve (FFR). *Math Model Nat Phenom 13(6): 57.* https://doi.org/10.1051/mmnp/2018069

14. Guerra T, Catarino C, Mestre T, Santos S, Tiago J, Sequeira A (2018) A data assimilation approach for non-Newtonian blood flow simulations in 3D geometries. *Applied Mathematics and Computation 321:176–194.* https://doi.org/10.1016/j.amc.2017.10.029

15. Gimel'farb G (2013) Image processing: Image filtering and segmentation. OMPSCI 373 Computer Graphics and Image Processing. https://www.cs.auckland.ac.nz/courses/compsci373s1c/PatricesLectures/2013/CS373-IP-03.pdf

16. Lopez-Palop R, Carrillo P, Agudo P, Frutos A, Cordero A, Lopez-Aranda M, Ramosc D (2013) Correlation Between Intracoronary Ultrasound and Fractional Flow Reserve in Long Coronary Lesions. A Three-dimensional Intracoronary Ultrasound Study. *Rev Esp Cardiol (Engl Ed) 66(9):707-14.* https://doi.org/10.1016/j.rec.2013.04.023

17. Pironneau O (2014) Simplified fluid-structure interactions for hemodynamics. *Numerical Simulations of Coupled Problems in Engineering 33:57-70.* https://doi.org/10.1007/978-3-319-06136-8_3

18. Boileau E, Pant S, Roobottom C, Sazonov I, Deng J, Xie X, Nithiarasu P(2017) Estimating the accuracy of a reduced-order model for the calculation of fractional flow reserve (FFR). *Int J Numer Method Biomed Eng 34:1.* https://doi.org/10.1002/cnm.2908

Author Alpha Estimating the accuracy of a reduced-order model for the calculation of fractional flow reserve (FFR) Int J Numer Method Biomed Eng